Surface-adsorbed long G-quadruplex nanowires formed by G:C linkages

T. Troha[1], I. Drevenšek Olenik[1,2], M. Webba da Silva[3], L. Spindler[4,2]

[1] Faculty of Mathematics and Physics, University of Ljubljana, Jadranska 19, 1000 Ljubljana, Slovenia
[2] Department of Complex Matter, "Jožef Stefan" Institute, Jamova 39, 1000 Ljubljana, Slovenia
[3] Biomedical Sciences Research Institute, University of Ulster, Coleraine, BT51 2SA, United Kingdom
[4] Faculty of Mechanical Engineering, University of Maribor, Smetanova 17, 2000 Maribor, Slovenia

Abstract

G-quadruplexes connected into long, continous nanostructures termed G-wires show properties superior to dsDNA when applied in nanotechnology. Using AFM imaging we systematically studied surface-adsorption of a set of G-rich oligonucleotides with GC-termini for their ability to form long G-wires through the G:C pairing. We investigated the effects of increasing sequence length, the type of nucleotide in the side loops, and removal of the CG-3' terminus. We found that sequences with adenine in the side loops most readily form G-wires. The role of magnesium as an efficient surface-anchoring ion was also confirmed. Conversely, as resolved from dynamic light scattering measurements, magnesium has no ability to promote G-quadruplex formation in solution. These insights may help selecting prosperous candidates for construction of G-quadruplex based nanowires and to explore them for their electronic properties.

Keywords: G-wires, G-quadruplex, (G:C:G:C) quartet, magnesium, AFM, dynamic light scattering.

1 Introduction

For a long time double-stranded DNA (dsDNA) was considered to be an optimal building block for molecular electronics. Its molecular recognition and self-assembling properties enable bottom-up organisation into nanoscale architectures. But a number of studies on different DNA-based systems failed to unambiougsly measure their electrical conductivity. Only recently, reproducible charge transport measurements in guanine-quadruplex DNA (G4-DNA) structures were reported [Livshits, 2014]. This finding is expected to renew the interest in DNA-based nanoelectronics.

Quadruplex DNA is formed from guanine-rich DNA molecules so that four guanine (G) residues associate via Hoogsteen hydrogen bonding into G-quartets (G4) (Figure 1a), while π-π stacking of G-quartets produces the quadruplex stem. When G-rich DNA or oligonucleotides self-assemble into long, continous quadruplex-based superstructures they are termed G-wires. These nanowires have mechanical properties superior to dsDNA in regard to potential use in nanocircuity: they resist enzymatic degradation and are mechanically and thermally stable [Kotlyar 2005, Yatsunyk 2013].

Transport measurements combined with theoretical modelling suggest that electrical transport in G4-DNA occurs by a thermally activated hopping between multi-quartet segments [Livshits 2014]. Due to this, it is essential to build G-wires with an unperturbed quadruplex stem. We recently showed that long G-wires can be constructed through cohesive self-assembly of GpC and CpG "sticky ends" [Maani Hessari, 2014]. In this arrangement GC-

overhangs are used to link two quadruplex stems via (G:C:G:C) quartets based on Watson-Crick G:C base pairing (Figure 1b). A model sequence d(GCGG**A**GGCG) was deposited on mica substrate to test the idea. Atomic force microscopy (AFM) proved the formation of several hundred-nanometer long wires with an average height of 1.7 nm, a value that is typical for G-quadruplexes when studied by AFM [Marsh 1995, Kotlyar 2005, Kunstelj 2007].

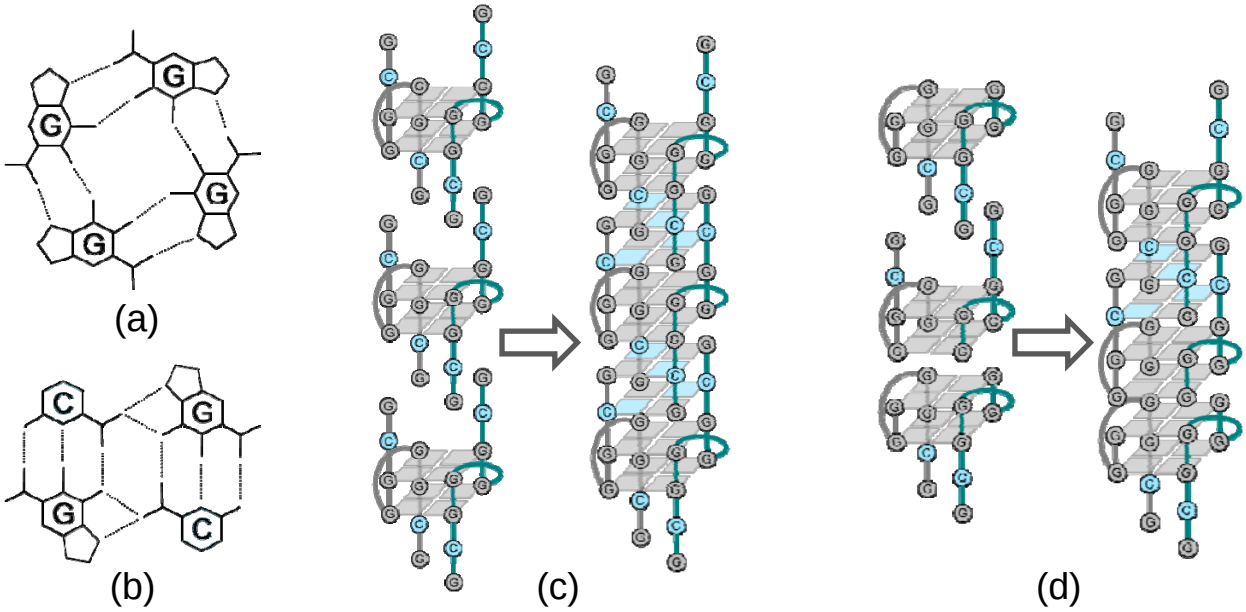

Figure 1. (a) Four guanine (G) residues form a planar G-quartet. (b) A (G:C:G:C) quartet [Webba, Biochem 2003]. (c) Bonding scheme of sequences containing both, 5' and 3' GC-ends. The basic building block is a bimolecular quadruplex with either A, T or TC in the side loops. (d) Bonding sequences without CG3' ends. G-wire growth at the 3'-end proceeds via terminal G-quartet stacking.

In this study we extend our previous work to find most suitable candidates for the formation of long, continuous G-wires. The previously used model sequence d(GCGG**A**GGCG) was altered by: (i) exchanging adenine (A) in the side loop with either thymine (T) or thymine-cytosine (TC), (ii) increasing the length of the oligonucleotide by increasing the number of repetitive (TG_4) segments in the GQ stem, (iii) removing a GC-overhang, and (iv) stimulating G-wire anchoring to mica with magnesium ions. Oligonucleotides were deposited onto freshly cleaved mica substrates by drop-coating from solution and the obtained surface structures were analysed with atomic force microscopy. We also tested the effect of magnesium ions on G-wire growth inside solutions by dynamic light scattering (DLS). Although not routinely used for studying the formation of G-quadruplexes, DLS can provide valuable information on quadruplex dimensions and their solution behaviour [Protozanova 2000, Wlodarczyk 2005, Spindler 2010, Zimbone 2012, Prislan 2012, Ilc 2013].

2 Materials and Methods

2.1 Materials

All oligonucleotides, except d(GCG_2**T**G_4**T**G_2CG), were purchased from Eurogentec (Seraing, Belgium) as 40 nM desalted syntheses and reconstituted in water. Oligonucleotides were folded by dialysis that was performed at a concentration of 100 µM DNA in the presence of 100 mM NaCl buffered with 10 mM sodium phosphate buffer (NaPi) at pH 6.8. The dialysed solutions were diluted to specified concentrations just prior to surface deposition. Oligonucleotide d(GCG_2**T**G_4**T**G_2CG) was purchased from Generi Biotech (Czech Republic) as a 4 mM aqueous solution desalted on a Sephadex G-25 column. It was diluted in 10 mM

NaPi buffer (pH 6.8) with 100 mM NaCl to the desired concentration to be used either for surface coating or dynamic light scattering. A small set of these solutions was additionally preincubated with 10 mM $MgCl_2$ to investigate the effect of magnesium ions on G-quadruplex formation in solution.

Table 1: Oligonucleotides used to study the effect of:

- sequence length	d(GCGG**T**G_4**T**GGCG), d(GCGG**T**G_4**T**G_4**T**GGCG), d(GCGG**T**G_4**T**G_4**T**G_4**T**G_4**T**GGCG)
- type of nucleotide in the side loop	d(GCGG**T**GGCG), d(GCGG**TC**GGCG), d(GCGG**A**GGCG)
- removing the 3'-CG overhang	d(GCGG**T**GG), d(GCGG**TC**GG), d(GCGG**A**GG)

2.2 AFM measurements

The procedure used for preparation of the surface films and then AFM imaging was in general following the protocol described by J. Vesenka [Vesenka, book 2011]. The samples were obtained by dropping of 5 µL of 20 µM oligonucleotide solution onto the substrate. After 15 minutes of drying, the excess material was removed by washing the substrate with distilled water. Then the sample was left to dry for at least one day at ambient conditions.
For the substrate, either freshly cleaved V-1 muscovite mica was used or mica coated with magnesium ions to promote nucleic acids binding. To coat the mica with Mg^{2+} cations, 500 µL of saturated $MgCl_2$ solution was deposited on a freshly cleaved mica sheet. After a short adsorption time the excess solution was removed with a pipette and the surface was washed with distilled water and dried at room temperature for at least 20 minutes.
AFM imaging was performed on a Veeco Dimension 3100 apparatus with a Nanoscope IV Controller (Veeco Metrology, Inc., Santa Barbara, CA). A silicon cantilever (OTESPA7) with resonance frequency of 320 kHz and tip radius between 3.6 and 5.6 nm was used. All the images were recorded in "Tapping mode" to minimize the contact with the surface architectures. The height distribution of the surface features was obtained with the Bearing function in Nanoscope software and analyzed by fitting a Gaussion curve to the obtained distribution function.

2.3 Dynamic light scattering

DLS experiments were performed on sequence d(GCG_2**T**G_4**T**G_2CG) which was diluted to a 1 mM concentration with a corresponding buffer. The setup consisted of an ALV-5000/60X0 Multiple Tau Digital Correlator (ALV-Laser Vertriebgesellschaft), a goniometer, and an avalanche photodiode detector. The light source was a frequency doubled Nd:YAG laser operating at $\lambda = 532$ nm. The scattered light was detected at scattering angles $40° \leq \theta \leq 130°$. The theoretical background of DLS investigations on G-quadruplex systems was described in detail previously [Spindler 2004, Włodarczyk 2005, Ilc JPCC 2013]. Two diffusive dynamic modes were observed in all measurements. The measured intensity autocorrelation functions were fitted to the following dependence [Mertelj 2009]:

(1)

where y_0 is the baseline correction, j_d the ratio between the intensity of the light that is scattered inelastically and the total scattered intensity, a_f the amplitude of the faster diffusive mode, and τ_i the relaxation time of the i-th diffusive mode. The stretch exponent parameter s_i, which can attain values $0 \leq s_i \leq 1$, is a qualitative measure of the width of the distribution of relaxation times. The value of s_i was usually close to 1 indicating a narrow distribution of relaxation times. The translational diffusion coefficient was obtained from the relation

$$D_i = 1/(\tau_i q^2) \quad (2)$$

where q is the scattering vector defined as $q = (4\pi n/\lambda)\sin(\theta/2)$, $n = 1.33$ is the solution refractive index, and λ the laser wavelength. From the diffusion coefficients the dimensions of

the scattering objects in solutions can be estimated. The corresponding hydrodynamic radius was calculated as

$$R_H = \frac{k_B T}{6\pi\eta D} \quad (3)$$

with k_B being the Boltzmann constant and η solvent viscosity. From the two diffusive dynamic modes the faster diffusive mode ($D_f \approx 10^{-10}$ m^2/s) is assigned to the diffusion of individual G-quadruplexes and their assemblies. The slower diffusive mode is assigned to large globular aggregates with hydrodynamic radii in the range of micrometers and is a typical feature of many polyelectrolyte systems including G-quadruplex solutions [Sedlak J Phys Chem 1996, Skibinska J Phys Chem 1999, Spindler JNA 2010, Zambone Eur. Biophys J 2012].

3 Results

Our previous work on solution assembly [Spindler, JNA 2010] showed that long oligonucleotides possessing several repeating GGGGT units formed larger assemblies. Polyacrylamide gel electrophoresis (PAGE) revealed that in the series d(GCG$_2$**T**G$_4$**T**G$_2$CG), d(GCG$_2$**T**G$_4$**T**G$_4$**T**G$_2$CG), and d(GCG$_2$**T**G$_4$**T**G$_4$**T**G$_4$**T**G$_4$**T**G$_2$CG), the later oligonucleotide exhibited the largest number of migrating bands with high molecular weight. To test if the same holds also for surface assembly, the same sequences were deposited onto freshly cleaved mica and investigated by AFM (Figure 2). Surprisingly, the two longest sequences showed no regular structures, just globular aggregates of variable height, between 2 nm and 6 nm. Only sequence d(GCG$_2$**T**G$_4$**T**G$_2$CG) formed bands of irregular shape, but with quite regular height h = (2.53 ± 0.15) nm suggesting possible quadruplex formation (Figure 2c).

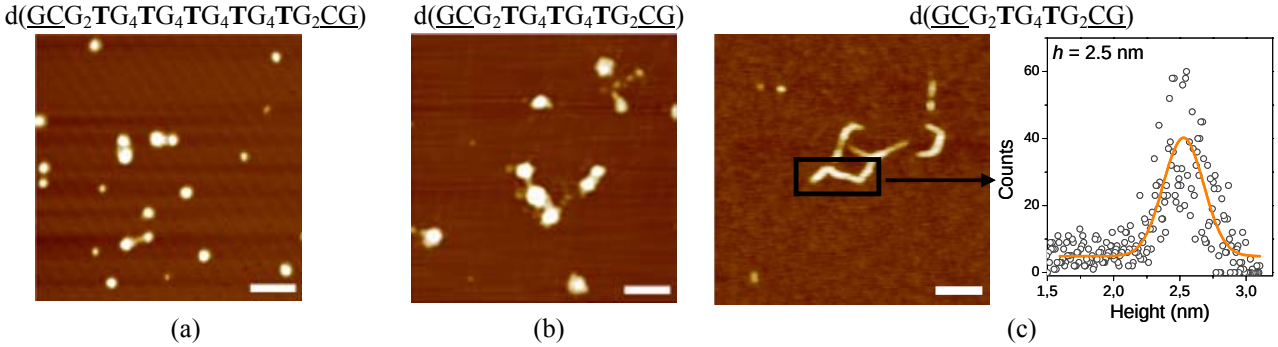

Figure 2. The effect of oligonucleotide length on G-wire formation. The scale bar in all images corresponds to 200 nm.

The model of G-wire formation via GC-sticky ends (Figure 1b) is independent of the nucleotide in the side loop. To test the validity of this hypothesis, adenine in the previously studied sequence d(GCGG**A**GGCG) [Ma'ani, 2014] was selectively exchanged by thymine or thymine-cytosine. Surface structures of the three sequences deposited on freshly cleaved mica differed considerably. Sequence d(GCGG**T**GGCG) formed only globules of varying size (Fig. 3.a), very similar to analogous longer oligonucleotides with thymine in side loops (Fig. 2.a.b). The sequence d(GCGG**TC**GGCG) showed more variable surface structures, sometimes connected by thin threads with a height of 1 nm or less (Figure 3b). In contrast, sequence d(GCGG**A**GGCG) formed wire-like structures up to 0.5 µm long. Interestingly, the wires appear to be of two different heights indicating structures with different diameters. The long rectilinear wire in Figure 2c, labelled with 1, has an average height of (1.10 ± 0.12) nm. The shorter and thicker wire, labelled 2, is notably higher with h = (1.72 ± 0.22) nm. While the value of 1.7 nm is less than the diameter of a typical quadruplex (2.8 nm), it coincides with the previously reported values for the same sequence [Nason, 2014], for G-wires from 5'-

GMP [Kunstelj, Colloids B, 2007] and also for sequence d(GGGGTTGGGG) [Marsh, JNA, 1995]. More puzzling are the 1.1 nm high wires, which can be attributed to some long range assemblies, but presumably with a different structure than the usual quadruplex-based wires.

Oligonucleotides with GC-overhangs are expected to form G-wires by (G:C) linkages between two successive quadruplexes. If one GC- terminal group is removed then a flat G-quartet terminates the quadruplex. Stacking of terminal G-quartets competes successfully with the formation of (G:C:G:C) linkages in the process of G-wire growth [Ilc, JPCC 2013]. We explored this possibility in surface growth by removing the terminal CG-3' ends from the previously studied set of oligonucleotides. The three new sequences: d(GCGG**T**GG), d(GCGG**TC**GG), and d(GCGG**A**GG), behave quite similarly to the sequences with both GC overhangs. The sequence with thymine forms globular structures of diverse height (Figure 3d), while sequence with TC-loops forms smaller globules and thread-like structures (Figure 3e). Only d(GCGG**A**GG) is capable of wire formation (Figure 3f), although these wires are shorter than observed for d(GCGG**A**GGCG). Again wires of two different heights are observed. Quite frequently these wires are at one end higher and broader and then become smaller and thinner. A detailed section analysis for one such wires is shown in Figure 3f. The average heights are (1.80 ± 0.01) nm and (1.35 ± 0.01) nm for the higher and lower part of the wire, respectively. The removal of the CG-3' overhang therefore does not substantially alter the surface structures of the investigated oligonucleotides.

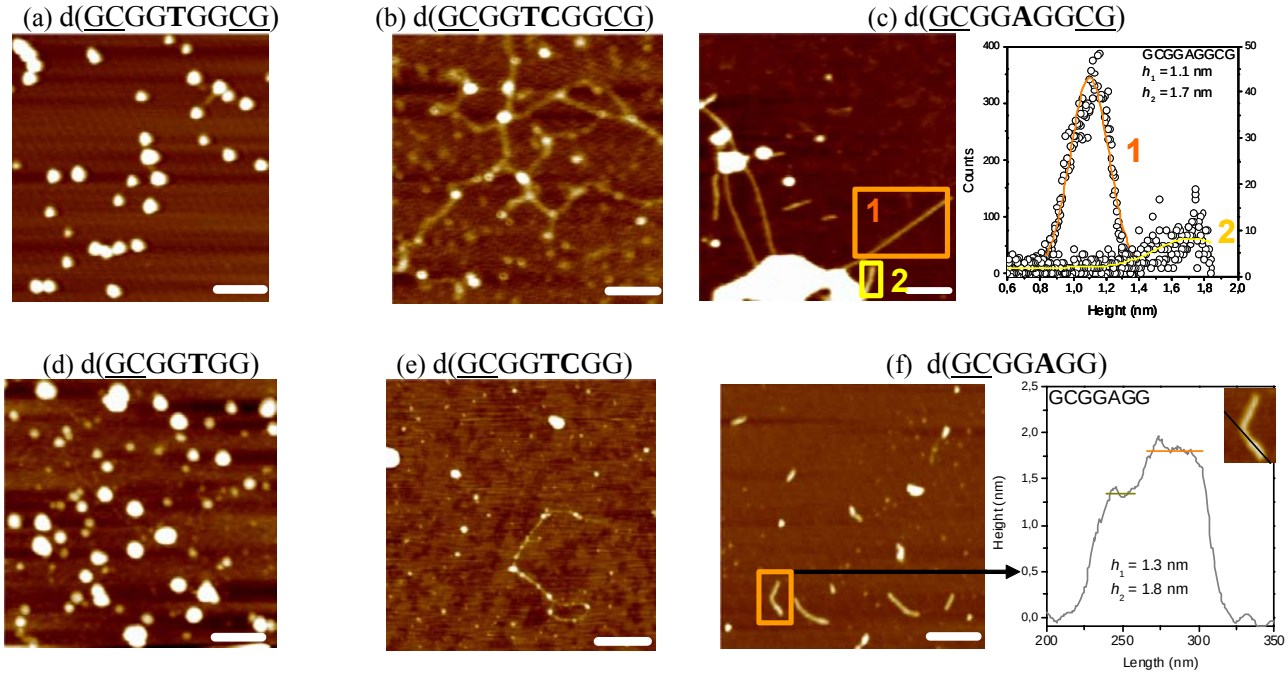

Figure 3. Effect of the nucleotide in the side loop and CG-3' removal on G-wire formation on freshly cleaved mica. Globular structures in (a) and (d) have variable heights between 2 and 7 nm, while the height of thin threads in (b) and (e) is below 1 nm. The scale bar in all images corresponds to 200 nm.

From Figures 2 and 3 it is evident that the investigated sequences exhibit a low adsorbtion tendency for freshly cleaved mica. To bind negatively charged DNA onto like-charged mica, divalent cations are standardly used, either by using them in the buffer or with a pretreated mica. The adsorption process is driven by the cooperative effect of divalent metal ion interaction with the mica surface groups, divalent metal ion condensation along DNA, and end-to-end DNA interactions [Hansma Biophys. J. 1996, Dahlgren 2002, Pastre Biophys. J.

2003, Song JPCB 2007, Lin Biomacromol. 2010]. Magnesium ions are generally preferred with respect to the transition metal cations that coordinate more strongly to the DNA bases.

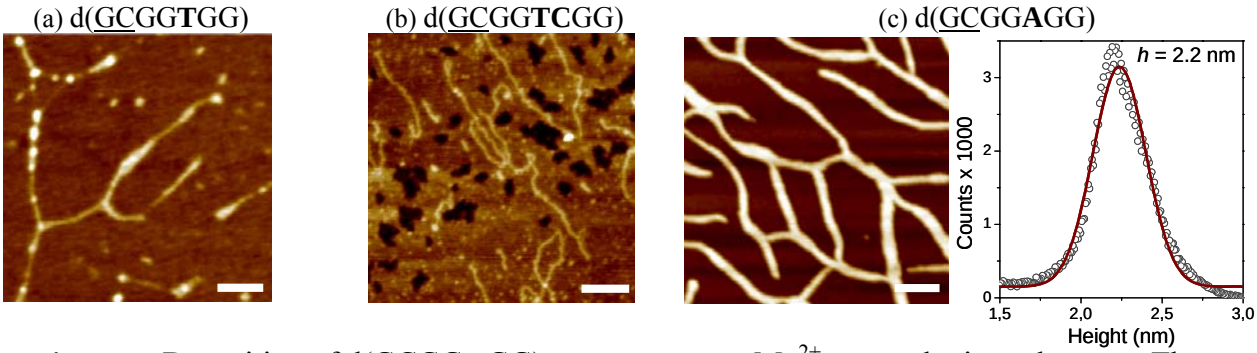

Figure 4. Deposition of d(GCGG**X**GG) sequences onto Mg^{2+} covered mica substrates. The height of most wires in (a) is below 1 nm, while the thin threads in (b) are uniformly high (0.8 nm). The wires observed in (c) exhibit a significantly larger height of 2.2 nm. The scale bar in all images corresponds to 200 nm.

We deposited a thin layer of Mg^{2+} ions on mica and repeated the surface deposition of d(GCGG**X**GG) sequences from Figure 3d-3f. Evidently, Mg^{2+} ions stimulated the formation of wire-like structures (Figure 4), but the height of these wires was different for each sequence, indicating a different assembling pattern. Sequence d(GCGG**T**GG) forms wires of variable height and width (Figure 4a), usually connecting some globular structures. The height of most wires is below 1 nm, but a few wires with an intermediate height of 1.3 nm are also formed. These could be interpreted as some soft quadruplex structures, probably with a folding topology different from the one proposed in Figure 1. For d(GCGG**TC**GG) wires of a more uniform height of about 0.8 nm are formed indicating that these structures are not quadruplexes, but rather single loosely bundled oligonucleotides (Figure 4b). Finally, sequence d(GCGG**A**GG) assembles into an interconnected network of wires with a well-defined height of (2.24 ± 0.16) nm (Figure 4c).

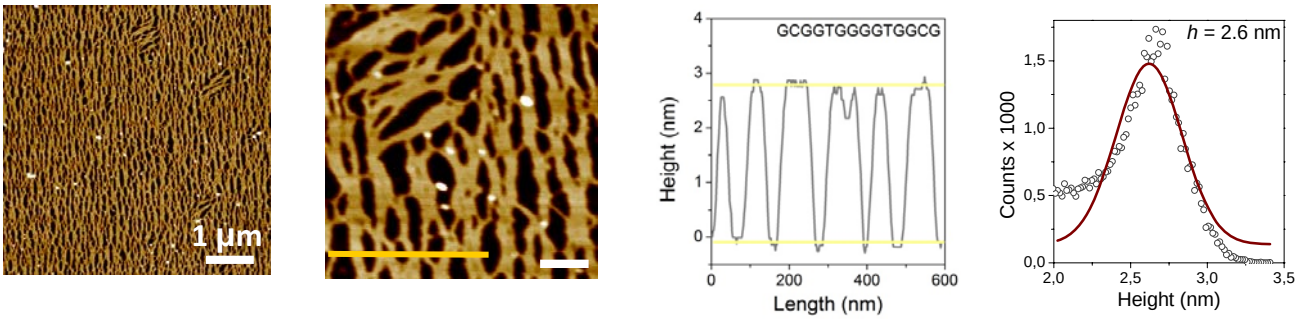

(a) (b) (c) (d)

Figure 5. Sequence GCG_2**T**G_4**T**G_2CG preincubated in 10 mM $MgCl_2$ and deposited onto freshly cleaved mica forms a large network of G-wires with a clear preferential direction (a). A cross-section along the yellow line in (b) shows a uniform height of the network (c), while the graph in (d) represents the height distribution of surface features in image (b).

To learn more about the effect of Mg^{2+} ions on G-wire formation, we added them to the buffering solution instead of depositing them directly onto mica. Mg^{2+} ions were previously found to effectively stimulate tethering of G-wires onto mica (Table 2). In our study, the sequence GCG_2**T**G_4**T**G_2CG was preincubated in 10 mM $MgCl_2$ and the samples were prepared following the usual procedure and deposited on freshly cleaved mica. Impressively, a formation of an extensive network of broad wires took place (Figure 5). These wires, although not really straight, exhibit a large-scale preferential direction. The main orientation

is only interrupted by a few patches of wires organised in a direction forming a 60° angle to the main direction (Figure 5a). This indicates that the general alignment of the structures follows the potassium vacancy sites of the underlying mica substrate [Vesenka, Cololids 2007; Kunstelj Colloids 2007]. A cross-section of the network taken along the orange line in Figure 5b clearly shows the well-defined height of the structures (Figure 5c). A complete analysis of Figure 5b gives the average value for the height distribution $h = (2.62 \pm 0.21)$ nm (Figure 5d), which is already close to the expected quadruplex diameter. In our last step, we combined both approaches: sequence GCG$_2$**T**G$_4$**T**G$_2$CG was preincubated in 10 mM $MgCl_2$ and then deposited on mica coated with the same ions. Again an extensive network of well organised wires was formed, very similar to the one shown in Figure 5 (data not shown).

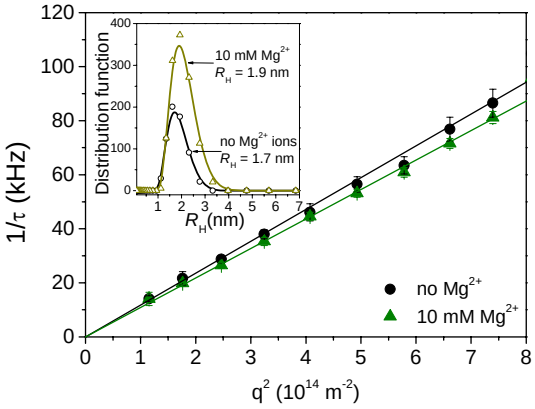

Figure 6. Dynamic light scattering results for 1 mM GCG$_2$**T**G$_4$**T**G$_2$CG prepared with or without 10 mM $MgCl_2$. Solid lines are fits to Equation (2). The inset shows the distribution function of the hydrodynamic radius for both solutions obtained from Equation (3). Both results suggest that magnesium ions have nearly no effect on quadruplex formation in solution.

As a final test, we investigated if Mg^{2+} ions induce G-wire formation already during preincubation in the $MgCl_2$ solution or rather during the deposition process. We used dynamic light scattering to study the size of scattering objects in a 1 mM GCG$_2$**T**G$_4$**T**G$_2$CG solution in the presence of 100 mM NaCl buffered with 10 mM NaPi (Figure 6). Measurements were taken for scattering angles between 40°and 130° and a translational diffusion coefficient of $D = (1.18 \pm 0.02) \cdot 10^{-13}$ m^2/s was calculated. The measurement was repeated for the same solution with an addition of 10 mM $MgCl_2$ and a similar value of $D = (1.09 \pm 0.01) \cdot 10^{-13}$ m^2/s was obtained. The slightly smaller value of D for magnesium containing solution could be attributed to additional screening coming from the extra cations, an effect typical for polyelectrolyte solutions [Schmitz book 1990, Liu J Chem Phys 1998]. DLS measurements were also visualised using the CONTIN algorithm [Provencher 1982] in ALV software. A distribution function for the relaxation times of the scattering objects was calculated and converted into the distribution function of the hydrodynamic radii of the two solutions (R_H = 1.9 nm if no Mg^{2+} is added and R_H = 1.7 nm with 10 mM Mg^{2+}) (insert in Figure 6). These results clearly demonstrate that Mg^{2+} ions do not stimulate G-quadruplex formation and G-wire growth inside a solution. It is rather their ability to bind oligonucleotides to mica that brings together a critical number of sequences needed to organize themselves into long G-wires.

4 Discussion

We investigated a number of short G-rich oligonucleotides with GC-overhangs to test their ability to form long G-wires on surfaces. Several conclusions can be drawn from our results and are summed up as follows:

4.1 Adenine works best

From all the investigated sequences, those having adenine in the side loop most readily formed organised structures even without the addition of magnesium ions. Sequence d(GCGG**A**GGCG) formed long rectilinear wires with lengths above 300 nm and apparent height of 1.1 nm. At the same time also shorter but higher h = 1.7 nm wires were observed. If the 3'CG-end was removed from this sequence, it was still able to form wires, but they were much shorter with lengths below 200 nm. Their height was either 1.3 nm or 1.8 nm and in some cases the wires have both heights. Upon addition of magnesium as a surface bridging ion, sequence d(GCGG**A**GG) formed a large network of broad bands of closely packed wires with and apparent height of 2.2 nm. In contrast, none of the sequences containing TC in the side loops formed quadruplex structures, not even on magnesium-coated mica. The flanking TC nucleotides seem to be too large to enable G-wire formation or for some reason, this kind of arrangement is not favored by surface adsorption.

4.2 Size does not matter

A set of sequences with increasing number of TG_4 runs was investigated, from d(GCGG**T**GGCG) (Figure 3a) all the way to d(GCGG**T**G_4**T**G_4**T**G_4**T**G_4**T**GGCG) (Figure 2). Unlike the previously performed PAGE study, in which the longest sequence formed the longest solution aggregates [Spindler, JNA 2010], there was no consistency in the formation of surface structures. Moreover, only sequence d(GCGG**T**G_4**T**GGCG) exhibited a limited number of organised structures with h = 2.5 nm without surface bonding magnesium. A similar comparative study was previously performed on sequences d($G_2T_2G_2$), d($G_4T_2G_4$) and d($G_6T_2G_6$) [Sondermann, 2002 AIP], but also there no proportionality between tendency for G4-wire formation and sequence length was observed, with only d($G_4T_2G_4$) readily forming G-wires.

4.3 Quadruplex formation and surface bonding with magnesium

As widely established, magnesium ions considerably promote surface anchoring of oligonucleotides. However, we found that they cannot induce G-quadruplex formation, if there is no intrinsic tendency for it. Sequences d(GCGG**T**GG) and d(GCGG**TC**GG) did not form organised structures on mica (Figure 3d-3e). When they were deposited on mica coated with magnesium, some oligonucleotides were bound to the substrate forming wires, but their height (< 1 nm) indicates that no quadruplex structures were formed (Figure 4a-4b). Sequence d(GCGG**A**GG), on the other hand, having an intrinsic tendency toward quadruplex formation as resolved in Figure 3f, developed a large network of G-wires when assisted by surface anchoring magnesium.

The effect of magnesium on surface bonding of G-wire forming oligonucleotides was additionally compared to its solution effect. As clearly evident from DLS measurements (Figure 6), the addition of 10 mM $MgCl_2$ into the buffering solution does not notably alter the diffusion coefficient or the hydrodynamic radius of the quadruplex structures in solution. This confirms that Na^+ or K^+ ions are needed as structure directing cations in the first place, and only after that Mg^{2+} can facilitate surface anchoring during the deposition process.

4.4 The problem of G-wire height

A number of different organised surface architectures were observed in our study exhibiting apparent heights of a considerable diversity. In literature, G-wire heights between 1.0 nm and

3.5 nm were reported (Table 2). These values depended on the method (AFM, STM), type of substrate (mica, gold, graphite), structure directing cations, and the use of Mg^{2+} for surface bonding. More recently, it was also established that strand directionality could influence G-wire stiffness [Borovok 2007 Anal. Biochem, Livshits 2014 Adv. Mater]. As a rule, the apparent height of G-wires on surfaces is generally smaller than the solution diameter of the quadruplex (2.8 nm), however, this effect is still much less pronounced than for dsDNA. While dsDNA partially unwinds and is pinned down to the substrate [Muir 1998], the quadruplex structures are expected to largely keep their shape. Some degree of quadruplex flattening is still expected to take place due to sample compression by the surface forces and the deformation from the tip pressure applied to the structures during AFM scanning. But, it is rather surprising that intra-molecular G4-DNAs with anti-parallel configuration were observed to have an apparent height of 1.0 – 1.1 nm, a value typically reported for dsDNA. This opens up the question, whether those nanowires really have the quadruplex structure as observed in the solution or does the structure change during surface deposition thus leading to some intermediate structures or alternative folds.

For the sequences with GC-overhangs, the observed apparent heights can be interpreted as:
(i) wires with 2.5 nm < h < 2.6 nm formed from d(GCGG**T**G_4**T**GGCG) are higher than most of other G-wires reported. This confirms their proposed bimolecular structure with a nucleotide in the side loops (Figure 1c) that results in a stiffer G-wire with and apparent height close to the solution diameter of 2.8 nm. This is additionally confirmed by the fact that the wire height is not notably affected by the presence of magnesium.
(ii) wires with 1.7 nm < h < 1.8 nm observed for d(GCGG**A**GGCG) and d(GCGG**A**GG) when no magnesium was added could still have the proposed structure. These sequences, however, are relatively short resulting in small quadruplexes. When assembled into G-wires such structures would appear softer and more easily deformable. The addition of Mg^{2+} buttresses the wires and their apparent height increases to 2.2 nm, indicating a stiffer structure.
(iii) wires with 1.1 nm < h < 1.3 nm fall in between quadruplex structures and single oligonucleotides laying on the surface (h < 0.9 nm). Such apparent heights signify some partially organised structures, for intance incompletely folded quadruplexes resulting from some intermediate structures frozen-in during the process of surface-deposition. Another possibility is that these surface structures have a different folding topology as the solution structures, since surface interactions and the addition of stabilising cations can be quite specific.

In general, our results signify that more importance should be given to the observed differences in the apparent heights of G-wires. The large variation in the values observed in our investigation as well as reported in the literature, 1.0 nm ≤ h ≤ 2.6 nm, cannot be just interpreted in terms of different experimental conditions, but the possibility of alternative folding patterns should be taken into account.

Table 2: Apparent height of G-wires from literature.

Sequence	Structure directing cation	substrate	Mg^{2+} for AFM deposition	wire height [nm]	ref.
5'-GMP	NH_4	mica	-	1.9	Kunstelj 2007
$G_4T_2G_4$	- Na K Na/spermidine	mica	yes	1.3 1.7 2.3 2.4	Marsh, NAR 1995
$G_4T_2G_4$	Na	mica	yes	2.2	Vesenka AIP 2002

$d(G)_{10}$	Na/K	graphite	-	1.5-3.5	Chiorcea-Paquim 2013
TG_4T	Na Na/K	graphite	-	2.1 1.9	Rodriguez-Pontinha 2014
GCG_2AG_2CG	Na	mica	-	1.7	Nason 2014
photonic DNA chromophore	K	mica	yes	1.5	Zhang 2013 Langmuir
monomolecular G-wires from poly(G) strands	K or no cation -	mica gold	yes -	1.0-1.2 1.2	Cohen 2007 Nano Lett Borovok 2008 Anal Biochem Roger-Eitan 2013 JPCC
biotin-avidin G4-DNA	-	mica gold	yes -	2.2 1.7	Borovok NAR 2008 Roger-Eitan 2013 JPCC

5 Conclusions

A large set of short G-rich oligonucleotides with GC-termini was systematically studied for their ability to form surface-adsorbed G-wires via (G:C) linkages. Our observations show, that the increased length of the oligonucleotide and the corresponding number of repeating (TG_4) units do not have stimulating effect on G-wire growth. This is quite in contrast to the solution behaviour of the same sequences observed previously by PAGE [Spindler JNA 2010]. Although a simple »GC sticky-ends« model suggests that the quadruplex fold and G-wire growth are independent of the nucleotide in the propeller loop, like in d(GCGG**X**GGCG), this nucleotide proved to play an important role in surface organisation. In general, adenine was found to enable G-wire formation in different sequences and even without the help of surface-anchoring magnesium ions. Thymine-cytosine pairs in the side loop, on the other hand, evidently disrupted the process of G-wire formation. This is again in contract to the solution aggregation studies [Mergny 2006 NAR]. G-wire growth through (G:C) connectivity was found to be equally effective as growth through terminal (G:G:G:G) stacking in sequences where the CG-3' end was removed (Figure 3). For any practical use as nanowires, though, the preferred mode of G-wire growth would be through an unperturbed quadruplex stem linked by G:C connections.

The effect of magnesium ions on G-wire growth was explored in detail. Magnesium was very effective in surface anchoring of the oligonucleotides, like is generally established. But, only those sequences that show formation of G-wires on freshly cleaved mica already without presence of magnesium, exhibit extensitve G-wire growth through magnesium as the bridging ion. Additionally, it was shown by dynamic light scattering measurements, that magnesium ions in solution do not induce G-wire growth. The effect of magnesium ions is therefore attributed to the surface anchoring of pre-formed quadruplexes in the process of solvent evaporation during surface deposition and substrate preparation. Finally, we observed a wide distribution of G-wire heights, from 1.1 nm to 2.6 nm, indicating different arrangements depending on the details of the molecular structure and substrate properties. This work represents a step towards designing new G4-DNA nanowires to be explored for their potential use in DNA-based nanoelectronics.

Acknowledgements
This work was supported by Slovenian Research Agency (Grant P1-0192).

References (alphabetical order)**:**

Natalia Borovok, Tatiana Molotsky, Jamal Ghabboun, Danny Porath, and Alexander Kotlyar, Anal. Biochem. **374**, 71-78 (2008). *Efficient procedure of preparation and properties of long uniform G4-DNA nanowires*.

N. Borovok, N. Iram, D. Zikich, J. Ghabboun, G. I. Livshits, D. Porath, A. Kotlyar, Nucleic Acids Research **36**, 5050-5060 (2008). *Assembling of G-strands into novel tetra-molecular parallel G4-DNA nanostructures using avidinbiotin recognition*.

Ana-Maria Chiorcea-Paquim, Paulina Viegas Santos, Ramon Eritja, and Ana Maria Oliveira-Brett, Phys. Chem. Chem. Phys. **15**, 9117-9124 (2013). *Self-assembled G-quadruplex nanostructures: AMF and voltammetric characterization*.

Hezy Cohen, Tomer Sapir, Natalia Borovok, Tatiana Molotsky, Rosa Di Felice, Alexander B. Kotlyar, and Danny Porath, Nano Lett. **7**, 981-986 (2007). *Polarizability of G4-DNA Observed by Electrostatic Force Microscopy Measurements*.

Paul R. Dahlgren, and Yuri L. Lyubchenko, Biochemistry **41**, 11372-11378 (2002). *Atomic Force Microscopy Study of the Effects of Mg^{2+} and Other Divalent Cations on the End-toEnd DNA Interactions.*

Helen G. Hansma, and Daniel E. Laney, Biophys. J. **70**, 1933-1939 (1996). *DNA Binding to Mica Correlates with Cationic Radius: Assay by Atomic Force Microscopy.*

Tina Ilc, Primož Šket, Janez Plavec, Mateus Webba da Silva, Irena Drevenšek-Olenik, Lea Spindler, J. Phys. Chem. C **117**, 23208-23215 (2013). *Formation of G-wires: The Role of G:C-base Pairing and G-quartet Stacking*.

Kotlyar, A. B.; Borovok, N.; Molotsky, T.; Cohen, H.; Shapir, E.; Porath, D. *Adv. Mater.* **2005**, 17, 1901–1905. *Long, Monomolecular Guanine-Based Nanowires.*

K. Kunstelj, F. Federiconi, L. Spindler, I. Drevensek-Olenik, Colloids and Surfaces B: Biointerfaces **59**, 120-127 (2007). *Self-organization of guanosine 5'-monophosphate on mica.*

Jing Lin, Yi-Yong Yan, Tian-Miao Ou, Jia-Heng Tan, Shi-Liang Huang, Ding Li, Zhi-Shu Huang, and Lian-Quan Gu, Biomacromolecules **11**, 3384-3389 (2010). *Effective detection and separation method for G-quadruplex DNA based on its specific precipitation with Mg^{2+}*.

H. Liu, L. Skibinska, J. Gapinski, A. Patkowski, E. W. Fischer, R. Pecora, J. Chem. Phys. **109**, 7556-7566 (1998). *Effect of electrostatic interactions on the structure and dynamics of a model polyelectrolyte. I. Diffusion*.

Gideon I. Livshits, Jamal Ghabboun, Natalia Borovok, Alexander B. Kotlyar, and Danny Porath, Adv. Mater **26**, 4981-4985 (2014). *Comparative Electrostatic Force Microscopy of Tetra- and Intra-Molecular G4-DNA*.

Gideon I. Livshits, Avigail Stern, Dvir Rotem, Natalia Borovok, Gennady Eidelshtein, Agostino Migliore, Erika Penzo, Shalom J. Wind, Rosa Di Felice, Spiros S. Skourtis, Juan Carlos Cuevas, Leonid Gurevich, Alexander B. Kotlyar, and Danny Porath, Nature Nanotechnology **9**, 1040-1046 (2014). *Long-range charge transport in single G-quadruplex DNA molecules*.

Nason Ma'ani Hessari, Lea Spindler, Tinkara Troha, Wan-Chi Lam, Irena Drevenšek-Olenik, and Mateus Webba da Silva, Chem. Eur. J. **20**, 3626-3630 (2014). *Programmed Self-Assembly of a Quadruplex DNA Nanowire*.

T.C. Marsh, J. Vesenka, E. Henderson, Nucleic Acids Research **23**, 696-700 (1995). *A New Dna Nanostructure, The G-Wire, Imaged By Scanning Probe Microscopy*.

J-L. Mergny, A. De Cian, S. Amrane, M. Webba da Silva, Nucleic Acids Res. **34**, 2386-2397 (2006). *Kinetics of double-chain reversals bridging contiguous quartets in tetramolecular quadruplexes*.

A. Mertelj, L. Cmok, M. Copic, Phys. Rev. E 79, 041402 (2009). *Anomalous diffusion in ferrofluids*.

Tera Muir, Emily Morales, Jeffrey Root, Indira Kumar, Brian Garcia, Christian Vellandi, Dena Jenigian, Thomas Marsh, Eric Henderson, James Vesenka, J. Vac. Sci. Technol. A **16**, 1172-1177 (1998). *The morphology of duplex and quadruplex DNA on mica*.

David Pastré, Olivier Piétrement, Stéphane Fusil, Fabrice Landousy, Josette Jeusset, Marie-Odile David, Loïc Hamon, Eric Le Cam, and Alain Zozime, Biophys. J. **85**, 2507-2518 (2003). *Adsorption of DNA to Mica Mediated by Divalent Counterions: A Theoretical and Experimental Study.*

Prislan, I.; Jamnik, A.; Tomšič, M. Kinetically Governed Formation of d($G_4T_2G_4$) Assemblies. *Acta Chim. Slov.* **2012**, *59*, 590–600.

E. Protozanova, R.B. Macgregor Jr., Biophysical Chemistry **84**, 137-147 (2000). *Thermal activation of DNA frayed wire formation*.

Stephen W. Provencher, Computer Physics Communication 27, 213-227 (1982). *A constrained regularization method for inverting data represented by linear algebraic or integral-equations*.

Ana Dora Rodrigues Pontinha, Ana-Maria Chiorcea-Paquim, Ramon Eritja, Ana Maria Oliveira-Brett, Anal. Chem. **86**, 5851-5857 (2014). *Quadruplex Nanostructures of d(TGGGGT): Influence of Sodium and Potassium Ions*.

Iris Roger-Eitan, Ke Liu, Gideon I. Livshits, Natalia Borovok, Dvir Rotem, Alexander B. Kotlyar, and Danny Porath, J. Phys. Chem. C **117**, 22462−22465 (2013). *High-Resolution Scanning Tunneling Microscopy Imaging of Biotin−Avidin−G4-DNA Molecules*.

K.S. Schmitz, *An Introduction to Dynamic Light Scattering by Macromolecules* (Academic Press, San Diego, 1990).

M. Sedlak, J. Chem. Phys. **105**, 10123-10133 (1996). The ionic strength dependence of the structure and dynamics of polyelectrolyte solutions as seen by light scattering: The slow mode dilemma.

L. Skibinska, J. Gapinski, H. Liu, A. Patkowski, E. W. Fischer, R. Pecora, J. Chem. Phys. **110**, 1794-1800 (1999). *Effect of electrostatic interactions on the structure and dynamics of a model polyelectrolyte. II. Intermolecular correlations*.

Anett Sondermann, Claudia Holste, Robert Möller, Wolfgang Fritzsche, AIP Conf. Proc. **640**, 93-98 (2002). *Assembly Of G-Quartet Based DNA Superstructures (G-Wires)*.

Yonghai Song, Cunlan Guo, Lanlan Sun, Gang Wei, Chongyang Peng, Li Wang, Yujing Sun, and Zhuang Li, J. Phys. Chem. B **111**, 461-468 (2007). *Effects of Bridge Ions, DNA Species, and Developing Temperature on Flat-Lying DNA Monolayers*.

L. Spindler, I. Drevenšek Olenik, M. Čopič, J. Cerar, J. Škerjanc, R. Romih, P. Mariani: *Dynamic Light Scattering and 31P NMR Spectroscopy study of the self-assembly of deoxyguanosine 5`-monophosphate the efect of added salt* , Eur. Phys. J. E **13**, 27-33 (2004).

Spindler, L.; Rigler, M.; Drevenšek-Olenik, I.; Ma'ani Hessari, N.; Webba da Silva, M. Effect of base sequence on G-wire formation in solution. *J. Nucleic Acids*, **2010**, Article ID 431651.

J. Vesenka, E. Henderson, T. Marsh, AIP Conf. Proc. **640**, 109-122 (2002). *Construction and examination of "G-wire" DNA*.

J. Vesenka, D. Bagg, A. Wolff, A. Reichert, R. Moeller, W. Fritzsche, Colloids And Surfaces B-Biointerfaces **58**, 256-263 (2007). *Auto-orientation of G-wire DNA on mica.*

James Vesenka, Preparation and Atomic Force Microscopy of Quadruplex DNA, Giampaolo Zuccheri and Bruno Samori (eds.), *DNA Nanotechnology: Methods and Protocols*, Methods in Molecular Biology, vol. 749, Springer Science+Business Media, LLC 2011.

M. Webba da Silva, Biochemistry **42**, 14356-14365 (2003). *Association of DNA quadruplexes through G : C : G : C tetrads. Solution structure of d(GCGGTGGAT)*.

A. Włodarczyk, P. Grzybowski, A. Patkowski, A. Dobek, J. Phys. Chem. B **109**, 3594-3605 (2005). *Effect of Ions on the Polymorphism, Effective Charge, and Stability of Human Telomeric DNA. Photon Correlation Spectroscopy and Circular Dichroism Studies*.

Liliya A. Yatsunyk, Olivier Piétrement, Delphine Albrecht, Phong Lan Thao Tran, Daniel Renčiuk, Hiroshi Sugiyama, Jean-Michel Arbona, Jean-Pierre Aimé, and Jean-Louis Mergny, Guided Assembly of Tetramolecular G-Quadruplexes. *ACS Nano* **2013**, *7*, 5701–5710.

Nan Zhang, Xiaozhu Chu, Maher Fathalla, and Janarthanan Jayawickramarajah, Langmuir **29**, 10796−10806 (2013). *Photonic DNA-Chromophore Nanowire Networks: Harnessing Multiple Supramolecular Assembly Modes*.

Zimbone, M.; Bonaventura, G.; Baeri, P.; Barcellona, M. L. Unusual Salt-Induced Behaviour of Guanine-rich Natural DNA Evidenced by Dynamic Light Scattering. *Eur. Biophys.* J. **2012**, *41*, 425–436.